CFIRE

AASHTO Mechanistic-Empirical Pavement Design Guide Parametric Study

CFIRE 03-24
March 2012

National Center for Freight & Infrastructure Research & Education
Department of Civil and Environmental Engineering
College of Engineering
University of Wisconsin–Madison

Authors:
Ruipeng Li and Steven Cramer
University of Wisconsin–Madison

Principal Investigator:
Steven Cramer
University of Wisconsin–Madison

DISCLAIMER

This research was funded by the National Center for Freight and Infrastructure Research and Education and the Wisconsin Highway Research Program of the Wisconsin Department of Transportation. The contents of this report reflect the views of the authors, who are responsible for the facts and the accuracy of the information presented herein. This document is disseminated under the sponsorship of the Department of Transportation, University Transportation Centers Program, in the interest of information exchange. The U.S. Government assumes no liability for the contents or use thereof. The contents do not necessarily reflect the official views of the National Center for Freight and Infrastructure Research and Education, the University of Wisconsin, the Wisconsin Department of Transportation, or the USDOT's RITA at the time of publication.

The United States Government assumes no liability for its contents or use thereof. This report does not constitute a standard, specification, or regulation.

The United States Government does not endorse products or manufacturers. Trade and manufacturers names appear in this report only because they are considered essential to the object of the document.

Wisconsin Highway Research Program

AASHTO Mechanistic–Empirical Pavement Design Guide Parametric Study

Institution: University of Wisconsin-Madison
Principal Investigator: Steven Cramer
Authors: Ruipeng Li and Steven Cramer
Date: March 2012

Technical Report Documentation Page

1. Report No. CFIRE 03-24	2. Government Accession No.	3. Recipient's Catalog No. **CFDA 20.701**	
4. Title and Subtitle **AASHTO Mechanistic-Empirical Pavement Design Guide Parametric Study**		5. Report Date **March 2012** 6. Performing Organization Code	
7. Author/s Ruipeng Li and Steven Cramer, University of Wisconsin-Madison		8. Performing Organization Report No. **CFIRE 03-24**	
9. Performing Organization Name and Address National Center for Freight and Infrastructure Research and Education (CFIRE) University of Wisconsin-Madison 1415 Engineering Drive, 2205 EH Madison, WI 53706		10. Work Unit No. (TRAIS) 11. Contract or Grant No. **DTRT06-G-0020**	
12. Sponsoring Organization Name and Address Research and Innovative Technology Administration United States Department of Transportation 1200 New Jersey Avenue, SE Washington, DC 20590		13. Type of Report and Period Covered **Final Report [1/1/2010 – 3/31/2012]** 14. Sponsoring Agency Code	
15. Supplementary Notes **Project completed for the Wisconsin DOT by CFIRE.**			
16. Abstract This study focuses on assessing the robustness of the AASHTO Mechanistic-Empirical Pavement Design Guide (MEPDG v 1.1) for rigid pavement design projects in Wisconsin. The primary tasks conducted in this study included performing sensitivity analysis on MEPDG's inputs for jointed plain concrete pavement (JPCP) design, evaluating the practicality of each input parameter's sensitivity, determining the effects of using different concrete materials and different hierarchical levels of inputs on predicted JPCP performances, and identifying the limitations of the current MEPDG. It was found that the coefficient of thermal expansion and modulus of rupture had a strong impact on MEPDG predictions and these outcomes appeared consistent with conventional wisdom. The adverse effects of the concrete unit weight and the positive benefits of the widened concrete slab were suspected to have been overestimated by the MEPDG. It was verified that MEPDG predictions were significantly different depending on the concrete materials and hierarchical levels of inputs chosen. Therefore, the pavement designer was recommended to select the proper design strategy. The limitations of MEPDG were illustrated in that it did not account for the effects brought by the supplementary cementitious materials on the pavement design and it erroneously restrained the permissible range for concrete modulus of rupture input. Although a significant number of material inputs are possible with level 1 implementation of the MEPDG, these inputs are often used in a narrow context and are largely independent from other inputs and material properties. It cannot be presumed that the change in one input will lead to a full set of parametric changes that such a change would actually induce in practice.			
17. Key Words Pavement Design Guide, MEPDG, AASHTO, Concrete, Coefficient of Thermal Expansion	18. Distribution Statement **No restrictions. This report is available through the Transportation Research Information Services of the National Transportation Library.**		
19. Security Classification (of this report) **Unclassified**	20. Security Classification (of this page) **Unclassified**	21. No. Of Pages 19	22. Price **-0-**

Form DOT F 1700.7 (8-72) **Reproduction of form and completed page is authorized.**

Table of Contents

Project Background

More economical and durable road construction has motivated the Wisconsin Department of Transportation (WisDOT) to consider implementing the new AASHTO Mechanistic-Empirical Pavement Design Guide (MEPDG). This guide is a computational tool for the new and rehabilitation pavement design utilizing a set of mechanistic and empirical models to predict the future performance of the pavements. In particular, major factors influencing the behavior and durability of a pavement, such as climate, traffic, and material characteristics are integrated within the considerations of the built-in models to obtain a precise prediction of performance and durability of pavements. The potential benefits of the MEPDG are to provide engineers and contractors with advanced tools and improvements in conservation, management, as well as significant economic savings.

The objectives of the project included installing and operating the MEPDG software to identify all the required data inputs, to assess the most sensitive inputs, and to identify MEPDG's limitations. The main parameters required by the MEPDG for the prediction of the new or rehabilitation design of Jointed Plain Concrete Pavement (JPCP), Continuously Reinforced Concrete Pavement (CRCP), and Portland Cement Concrete (PCC) overlay include information on traffic, climate, and pavement structure. Particularly for the pavement structure inputs, pavement layer design and material characteristics are specified. Detailed descriptions of each input part are included in Appendix A.

Research Task

1. Software installation

The MEPDG v1.1 installation software and the climatic files for the entire country were downloadable from the NCHRP website (NCHRP Design Guide, Mechanistic-Empirical Design of New & Rehabilitated Pavement Structures. http://onlinepubs.trb.org/onlinepubs/archive/mepdg/home.htm). The climatic files were installed in the same directory used for the MEPDG installation, allowing the MEPDG software to access the weather station data for pavement design.

2. Identification of Variables Required for Pavement Design

Four categories of design inputs are required by MEPDG, which are general inputs, traffic inputs, climate inputs, and material characterization inputs. General inputs include site-specific information and analysis reliability information. Inputs within this part deal with pavement site conditions, selected design parameters for evaluation purpose, and the corresponding reliability for each design parameters. Traffic inputs include traffic volume information, wheel load information, and traffic adjustment factors. Climatic information from the selected weather station database and the water table depth at the construction site are required inputs for the climate section. The climatic factors that affect pavement design include temperature and moisture, causing PCC slabs to curl and warp. Material characterization inputs include basic material properties for computing pavement response and distress (Guide for Mechanistic-Empirical Design of New and Rehabilitated Pavement Structures. National Cooperative Highway Research Program, Transportation Research Board, National Research Council, 2004).

This report is mainly focused on researching the influences of material property changes of the Portland Cement Concrete (PCC) Layer on predicted JPCP performances by MEPDG. Such material properties include basic ones for computing pavement responses such as PCC elastic modulus and Poisson's ratio, additional ones for the distress/transfer functions such as PCC modulus of rupture and tensile strength, and others for climate model, such as index properties and thermal properties. PCC

modulus of rupture and modulus of elasticity are the key parameters for the MEPDG to calculate JPCP distress and response. Three hierarchical levels are permitted for obtaining these two parameters. The Level 1 option requires direct measurements of them at 7, 14, 28, and 90 day. The Level 2 option requires direct measurements on concrete compressive strength at 7, 14, 28, and 90 day and then it converts the compressive strength results to the corresponding modulus of elasticity and modulus of rupture results. The Level 3 option requires only one measurement or an estimation of the concrete 28-day compressive strength value or modulus of rupture value. It utilizes empirical relations to first convert the 28-day modulus of rupture result to the corresponding modulus of rupture results at 7, 14, and 90 day. These results are further converted to compressive strength values at the same dates. The same empirical relations used in level 2 option are used to acquire the corresponding modulus of elasticity results (Guide for Mechanistic-Empirical Design of New and Rehabilitated Pavement Structures. National Cooperative Highway Research Program, Transportation Research Board, National Research Council, 2004). Detailed descriptions of the three levels of input options are shown in Appendix B.

3. Sensitivity Analysis

Three design parameters are proposed for JPCP design, which are transverse cracking, mean transverse faulting, and IRI. All of these design parameters must be satisfied at the specified reliability levels for a passed acceptable pavement design by MEPDG. Transverse cracking (unit, %) is defined as the ratio of the total number of transverse cracks across the breadth of slabs to the total number of slabs. Mean transverse faulting (unit, in) is defined as the average elevation difference between two adjacent slabs at the transverse joints for the entire pavement. IRI is the abbreviation for international roughness index, a parameter used to reflect the pavement surface smoothness condition, measured by in/mile. A high value of IRI denotes a highly deteriorated pavement surface (Guide for Mechanistic-Empirical Design of New and Rehabilitated Pavement Structures. National Cooperative Highway Research Program, Transportation Research Board, National Research Council, 2004). The sensitivity analysis conducted in the following section is to quantitatively relate the change of each individual input to the change of the design parameters. The inputs for the standard JPCP design are shown in Appendix C.

3.1. Single-Variable Sensitivity Analysis

To quantify the sensitivity of each variable, ‘y’ was defined as the relative percentage change of a predicted performance (design parameter) due to the relative percentage change of an input. For example:

$$y_{cracking} = \frac{\Delta cracking}{initial\ cracking}$$

$$y_{faulting} = \frac{\Delta faulting}{initial\ faulting}$$

$$y_{IRI} = \frac{\Delta IRI\ increment}{initial\ IRI\ increment}$$

where:
$\Delta cracking$: cracking increment;
$initial\ cracking$: cracking of the standard design;
$\Delta faulting$: faulting increment;
$initial\ faulting$: faulting of the standard design;
$\Delta IRI\ increment$: the new predicted IRI increment minus the standard trial design’s IRI increment;
$initial\ IRI\ increment$: the standard trial design’s IRI increment;
The expression for calculating IRI change was different because the PCC slab had an initial non-zero IRI value.

The variable 'x' was defined as the relative percentage change of an input. For example, the x expression for the compressive strength was:

$$x_{fc'}=\frac{\Delta fc'}{fc'}$$

where:
$\Delta fc'$: change of the input fc';
fc': the input fc' used in the standard JPCP trial design;

Sample inputs for sensitivity analysis are shown in Appendix C. For each variable selected for sensitivity analysis, a trend line was constituted by the data points of x versus y. The lower limit of y is -1, corresponding to the situation when the new predicted pavement performance (for example, cracking) is zero. The upper limit of y is unknown and could be a very large number. A typical x vs. y relation is shown in the Figure 1. It is observed that y increases rapidly when x is positive, and approaches -1 for negative x values. The shape shown in Figure 1 is analogous to the form of an exponent function, but it is possible that the shape of x versus y relation is close to a linear form for very insensitive inputs. Therefore, two forms of fitting curves were proposed to simulate each variable's sensitivity, which were$y = A \cdot B^x + C \cdot x + D$, a hybrid form with unknown values for A, B, C, and D, or $y = A \cdot B^x + C$, an exponent form with unknown values for A, B, and C. Based on the comparison of the two fitting curves, $y = A \cdot B^x + C$ was selected to simulate each variable's sensitivity due to higher accuracy. (Details are shown in Appendix D)

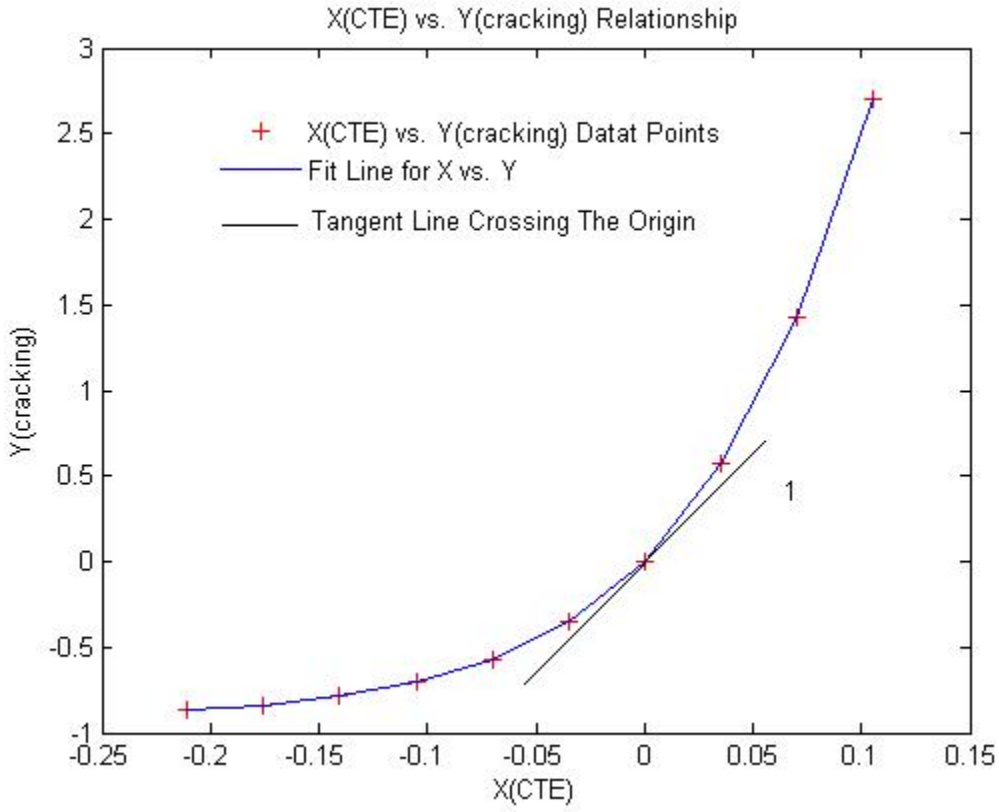

Figure 1 $y_{cracking}$ vs. x_{CTE} relationship

The sensitivity of a variable is defined as the change of the output due to a unit change of an input, which is expressed as the slope of the line crossing the origin, the point corresponding to the input and the output of the standard JPCP design. The example involving the definition of the sensitivity of CTE is shown in Figure 1, where line 1 is the tangent line crossing the origin. Sensitivity of CTE was

expressed as the slope of line 1. The slope of the tangent line for any variable could be either positive or negative. A positive slope value meant that an increase of the specified input would cause the increase of the corresponding predicted output, and vice versa. For comparison purpose, the magnitude of a variable's sensitivity was determined as the absolute value of the tangent line's slope. Detailed sensitivity analysis results are shown in Table 1:

Table 1 Sensitivity Analysis Results for JPCP

		Tangent Slope			Sensitivity		
Variables		Cracking	Faulting	IRI	Cracking	Faulting	IRI
Traffic	AADTT	1.963	0.417	0.342	S	LS	LS
	Mean Wheel Location	-3.377	-0.719	-0.610	S	MS	MS
	Truck Percentage	1.945	0.496	0.383	S	LS	LS
	Traffic Wander	1.621	0.330	0.263	S	LS	LS
Structure	Dowel Diameter	0.000	2.719	-1.767	NS	S	S
	Dowel Spacing	0.000	0.000	0.000	NS	NS	NS
	Lose Full Friction Time	0.169	0.000	0.005	LS	NS	NS
	Thickness	-17.950	-0.124	-1.127	ES	LS	S
	Cement Content	-0.075	0.229	0.149	NS	LS	LS
	w/c ratio	-0.065	0.114	0.111	NS	LS	LS
Level 1	7-day MR	1.707	0.000	0.072	S	NS	NS
	14-day MR	0.227	0.000	0.006	LS	NS	NS
	28-day MR	-16.650	-0.069	-1.231	ES	NS	S
	90-day MR	-6.177	0.000	-0.235	VS	NS	LS
	7-day E	-1.589	-0.086	-0.118	S	NS	LS
	14-day E	0.000	0.000	0.000	NS	NS	NS
	28-day E	9.743	0.086	0.416	VS	NS	LS
	90-day E	3.716	0.207	0.291	S	LS	LS
Level 2	7-day fc'	0.000	-0.026	-0.027	NS	NS	NS
	14-day fc'	0.143	0.000	0.006	LS	NS	NS
	28-day fc'	-7.754	0.000	-0.357	VS	NS	LS
	90-day fc'	-0.549	0.103	0.044	LS	LS	NS
level 3	28-day fc'	-8.415	0.059	-0.306	VS	NS	LS
Other Properties	CTE	12.241	2.210	1.921	ES	S	S
	Unit Weight	18.721	-2.733	-1.150	ES	S	S
	Poisson's Ratio	3.076	0.388	0.353	S	LS	LS
	Thermal Conductivity	-17.270	-0.416	-0.811	ES	LS	MS
	Heat Capacity	-0.221	-0.095	-0.104	LS	NS	LS
	Time to develop 50% Shrinkage	0.000	0.000	0.000	NS	NS	NS
	Reversible Shrinkage	-0.068	0.000	0.000	NS	NS	NS

Note: "Slope" shown below is short for "Absolute Value of the Tangent Line's Slope".

1. Slope>10: Extremely Sensitive (ES)
2. 5< Slope ≤10: Very Sensitive (VS)
3. 1< Slope ≤5: Sensitive (S)
4. 0.5< Slope ≤1: Moderately Sensitive (MS)
5. 0.1< Slope ≤0.5: Lowly Sensitive (LS)
6. Slope ≤0.1: Not Sensitive (NS)

It is observed that the cracking prediction was sensitive to most of the inputs, especially for pavement thickness, concrete coefficient of thermal expansion (CTE), and PCC unit weight. Concrete cracks when the tensile stress exceeds its cracking capacity. Based on the loading location, the maximum

tensile stress of the concrete pavement due to bending occurs at either the top surface or the bottom. Due to the fact that the traffic loads are repetitive, fatigue damage governs for pavement cracking. The pavement's cracking capacity is a deducted value below the concrete's maximum tensile strength, depending on the cycles of the loads. Tensile stress at the bottom or the surface of the pavement is defined in equation 1:

$$\sigma = \frac{M}{S} \quad \text{(Equation 1)}$$

M is bending moment and S is the section modulus, which is proportional to the second power of pavement thickness. As a result, pavement thickness is identified as an extremely sensitive input. Concrete Modulus of Rupture is a parameter representing the pavement's cracking capacity; hence it is identified as a very sensitive input.

Curling stress is proportional to the concrete coefficient of thermal expansion. For concrete with a high CTE value, the curvature of the pavement could be very large (Figure 2). While slab is in full contact with base, the real curvature is zero. This is equivalent to imposing a moment reversely. The higher the CTE value, the higher the pavement thickness, the higher this equivalent bending moment. This relation is illustrated in Equation 2:

$$\frac{\alpha \cdot \Delta t}{h} = \frac{1}{\rho} = \kappa = \frac{M}{EI} = \frac{M}{E \cdot \frac{1}{12} b h^3} \quad \text{(Equation 2)}$$

α is the concrete CTE value, h is the pavement thickness, κ is the curvature, E is the concrete modulus, and M is the equivalent bending moment. This process occurs when the slab has not separated from base. When the slab has lost full contact with base, a similar process occurs, shown in Equation 3. Therefore, it is reasonable that CTE is an extremely sensitive input.

Unit weight is identified as the most sensitive parameter for cracking prediction, which is beyond expectation. Based on Figure 2, stress caused from pavement self weight will combine with stress from traffic loads when the PCC slab loses full contact with subbase. This process will occur far beyond the time when the pavement is constructed, shown in Equation 3 for the upper case of Figure 2. As long as the pavement is still in full contact with base, the slab's self weight will not contribute to the tensile stress.

$$M = \frac{1}{8} q l^2 = \frac{1}{8} \gamma b h l^2 \quad \text{(Equation 3)}$$

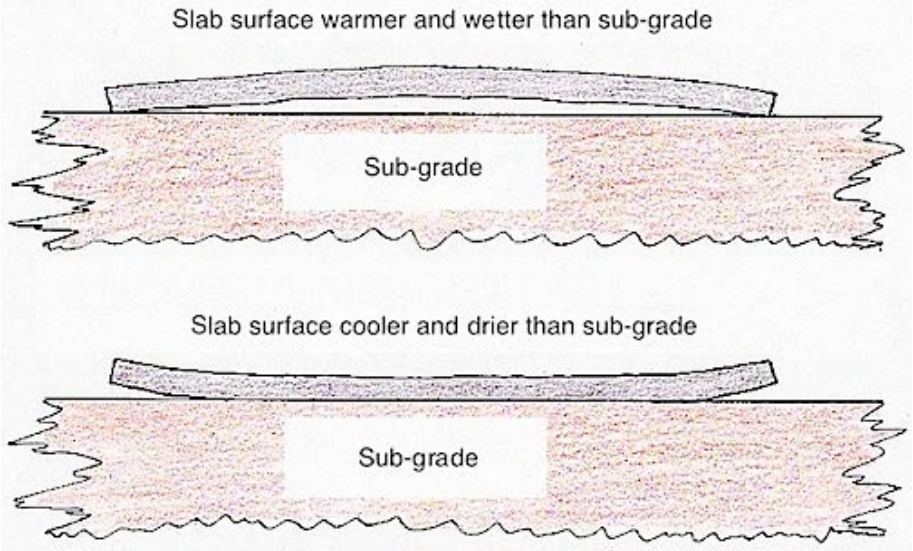

Figure 2 Concrete Slab Curl

γ is the concrete unit weight, b is the slab width, h is the slab thickness, and l is the slab length. For the typical concrete whose unit weight ranges from 140 to 150 pcf, and the common pavement with 10 inches thickness and 12 feet width, the moment caused by self-weight is at most 42.2 kip-ft at the mid-section. While for a standard single axle load (18 kips) applied at the mid-section, the corresponding bending moment at the mid-section is 67.5 kip-ft. Considering the moment caused by self-weight is far less repetitive than the one caused by traffic loads, and the single axle load is only the minimum one, moment induced by the slab's self weight should not cause a significant problem for pavement performance. Furthermore, the trend for the slab to completely separate from the base is restrained by dowels. Considering the damage from the slab's self weight is much lower than the one from traffic load, yet AADTT is not a very sensitive parameter, it is hypothesized here that the role of unit weight is magnified in the cracking model.

Figure 3 Joint Faulting Diagram

It is also observed that the faulting prediction is not sensitive to most of the inputs. This is possibly due to the calibration of the faulting model. Faulting predictions are not always improved (decreasing) with the increase of thickness. When the pavement is very thick, the faulting performance deteriorates. In reality, faulting is the deflection of the slab at the location of the joint. Shown in Figure 3, the worst case is that a point load (P) is applied at the slab corner. For simplicity, dowels are neglected and the slab's deformation due to load P is calculated in Equation (4).

$$\delta = \int \frac{\bar{M} \cdot M}{EI} = \int_0^{\frac{s}{\sqrt{2}}} \frac{P \cdot x \cdot x}{E \cdot \frac{1}{12} \cdot 2x \cdot h^3} dx = \frac{3Ps^2}{2Eh^3} \quad \text{(Equation 4)}$$

s is the length affected by the point load P, E is the concrete modulus of elasticity, and h is the slab's thickness. Based on Equation (4), the slab's deflection is inversely proportional to the third power of slab's thickness. Therefore, faulting should be very sensitive to slab's thickness, rather than insensitive to it.

The IRI predictions are not sensitive to most of the listed variables either. The reason could be due to the calibration of the IRI model. As a parameter representing the smoothness condition of the pavement, the fact that it is not sensitive to Annual Average Daily Truck Traffic (AADTT, a parameter representing the traffic volume) is beyond expectation. It is the traffic that gradually causes the deterioration of the pavement surface.

Inputs such as shoulder option, joint type, and aggregate type, are not expressed numerically, so the above quantitative method is not applicable for evaluating their sensitivities. It was found that all the three design parameters were extremely sensitive to slab width, so it is also listed separately. The changes of these inputs and the corresponding pavement performance predictions are shown in the following tables.

Based on the results shown in Table 2, the MEPDG manifests that the use of a widened slab could significantly improve the pavement performances by greatly decreasing the predicted cracking and faulting. It is believed that by using the widened slab, the wheel location is moved away from the shoulder. There is a significant difference between the use of a 12-ft slab and the use of a 13-ft slab, but little difference between the use of the 13-ft slab and 14-ft slab. Typically a slab is widened to 14 feet. Considering the 13-ft slab can significantly improve the pavement performances while the 14-ft slab does not show any additional significant improvements, it seems that the built-in models unrealistically overestimate the benefits of the widened slab.

Table 2 Relation between Predicted Pavement Performances and Slab Width (Widened Slab)

Slab Width/ft	cracking, %	faulting, in	IRI, in/mile
12	3.7	0.116	168.9
13	0.1	0.038	124.9
14	0.1	0.033	122.1

Both tied and untied shoulders are different options for pavement shoulder design. For tied shoulders, different values of long term load transfer efficiency (LTE) are further specified. From the results shown in Table 3, the use of ties can improve the predicted pavement performances. Such benefits are proportional to the increase of LTE.

Table 3 Relation between Predicted Pavement Performances and Shoulder Type

	Untied	Tied						
LTE	0%	20%	30%	40%	50%	60%	70%	80%
cracking, %	3.7	2.3	1.3	0.8	0.5	0.3	0.2	0.1
faulting, in	0.116	0.112	0.108	0.104	0.1	0.097	0.093	0.09
IRI, in/mile	168.9	165.6	162.7	160.2	158	156	154.1	152.4

Various joint sealant types are available for JPCP design. In MEPDG, two options for sealant are specified, which are preformed sealant and other sealant, including liquid sealant and no sealant. Based on the results shown in Table 4, it is observed that there is little difference on predicted pavement performances due to different joint sealant types. Therefore, the benefits brought by the sealant are not directly considered by MEPDG.

Table 4 Relation between Predicted Pavement Performances and Joint Sealant Type

Joint Sealant Type	cracking, %	faulting, in	IRI, in/mile
Preformed	3.7	0.116	165.7
Other	3.7	0.116	168.9

Though an essential parameter for concrete mix design, results in Table 5 show that different coarse aggregate types do not directly affect the predicted pavement performances. This is because coarse aggregate type is used only to determine the ultimate shrinkage at 40% relative humidity. In MEPDG's internal processing, it has no effect on concrete strength inputs or thermal inputs (Guide for Mechanistic-Empirical Design of New and Rehabilitated Pavement Structures. Final Report. National Cooperative Highway Research Program, Transportation Research Board, National Research Council, 2004).

Table 5 Relation between Predicted Pavement Performances and Aggregate Type

Aggregate Type	cracking, %	faulting, in	IRI, in/mile
Dolomite	3.7	0.116	168.9
Limestone	3.7	0.116	168.9
Quartzite	3.7	0.116	168.9
Rhyolite	3.7	0.116	168.9
Granite	3.7	0.116	168.9

3.2. Effects on Pavement Thicknesses due to Concrete Materials

Concrete component material properties, including but not limited to: cementitious material content, water to cement ratio, and coarse aggregate type, were not identified as sensitive variables in the above sensitivity analysis. This lack of sensitivity directly contradicted with laboratory observations and research investigations that concrete mechanical and thermal properties were sensitive inputs for MEPDG and dependent on concrete component properties (Ruipeng Li, 2011). This contradiction was because these inputs are only used in a very simplistic manner by the program and the obvious correlations between materials and properties are largely ignored.

To investigate the effects of concrete component material properties on rigid pavement performances using MEPDG, it is necessary to establish the relationships between concrete component material properties and concrete mechanical/thermal properties. The effects of the concrete component material properties' changes on pavement performances were reflected by the changes of concrete mechanical/thermal properties. The latter were identified as sensitive inputs and substituted into MEPDG in the trial design.

Within the scope of this research, it is hypothesized that different concrete components only affect the following concrete properties: modulus of elasticity, modulus of rupture, coefficient of thermal expansion, compressive strength, unit weight, and Poisson's ratio. For the analysis within this section, when one of the concrete component properties was changed, these mentioned concrete mechanical/thermal properties were updated based on experimental observations on concrete mixes and substituted into MEPDG to calculate the critical pavement thickness due to this change (The rest of the inputs remained the same as those shown in Appendix C). For JPCP design, design parameters such as

cracking, faulting, and IRI must be all satisfied at the corresponding reliability level for a passed design. The required pavement thickness when at least one of the design parameters was just satisfied at the specified reliability level was selected as the critical thickness.

Results from Table 6 were used to evaluate the effects on required pavement thicknesses due to different coarse aggregate sources (comparisons among rows) and due to using different supplementary materials (comparisons among columns). Observed from Table 6, pavement thickness varies with coarse aggregate source. Moreover, the use of supplementary materials, especially slag, basically improves the rigid pavement's performance by decreasing the required pavement thickness.

Table 6 Effect Due to Different Aggregate Type and the Use of Supplementary Materials

	Normal Mix		Slag 1		Fly Ash 1	
Coarse Aggregate Source	Mix#	Thickness, in	Mix#	Thickness, in	Mix#	Thickness, in
GG1 (dolomite dominant)	1	9.3	16	8.2	31	8.4
GG3 (granite dominant)	3	8.5	18	8.6	33	8.5
GG6 (dolomite dominant)	6	9.1	21	8.3	36	8.2
CS1 (dolomite dominant)	7	8.9	22	7.8	37	8.6
CS4 (dolomite dominant)	10	8.5	25	7.7	40	8.2
CS6 (quartzite dominant)	12	9.5	27	8.6	42	8.6
CS7 (basalt dominant)	13	8.7	28	8.0	43	8.3

Results from Table 7 were used to evaluate the effects on predicted pavement thicknesses due to different cement sources. The two different sources of cement were used and denoted as Cement I and Cement II. Based on the critical thickness comparisons within Table 7, for most cases, the use of the same type of cement manufactured in different places does not affect the pavement thickness.

Table 7 Effect Due to Different Sources of Cement

Cement I		Cement II	
Mix#	Thickness, in	Mix#	Thickness, in
16	8.2	46	7.9
22	7.8	48	8.1
32	9.1	57	8.8
37	8.6	58	7.4
71	8.4	51	8.1
72	8.6	52	7.6
77	8.4	62	8.1
81	9.3	66	8.5
73	7.8	53	7.6
78	8.0	63	8.3
83	8.0	68	8.0

Results from Table 8 were used to evaluate the effects of different types of slag on the required pavement thicknesses. The first column lists all the selected concrete mixes using Grade 120 slag. The third column lists all the corresponding concrete mixes using Grade 100 slag served as the counterpart. Based on the results shown in Table 8, the difference of required pavement thicknesses caused by the use of different types of slag was very small. Therefore, different types of slag do not affect the required pavement thicknesses.

Table 8 Effect Due to Different Sources of Slag

Slag 1, Grade 120		Slag 2, Grade 100	
Mix#	Thickness, in	Mix#	Thickness, in
16	8.2	71	8.4
22	7.8	73	7.8
24	8.1	75	8.1
46	7.9	51	8.1
47	7.4	52	7.6
48	8.1	53	7.6
50	7.7	55	7.7

Results from Table 9 were used to evaluate the effect due to the use of different sources of fly ash on critical pavement thicknesses. Concrete mixes listed in each row had the same mix design except for different sources of fly ash (FA1, FA2, and FA3) used. Concrete mixes listed in the same column were different mixes using the same fly ash. Observed from the results in Table 9, the pavement's critical thickness corresponding to each of the source of fly ash is considerably different. In other words, the source of fly ash had a considerable effect on predicted pavement thickness.

Table 9 Effect Due to Different Sources of Fly Ash

FA1		FA2		FA3	
Mix#	Thickness, in	Mix#	Thickness, in	Mix#	Thickness, in
31	8.4	76	9.0	81	9.3
32	9.1	77	8.4	82	8.3
37	8.6	78	8.0	83	8.0
56	8.4	61	8.7	66	8.5
58	7.4	63	8.3	68	8.0

Results from Table 10 were used to evaluate the effect on required pavement thickness due to using different sources of fine aggregate, denoted as sand A and sand B. Concrete mixes listed in the same row have the same mix design except for the different fine aggregate source. Concrete mixes listed in the same column are different mixes using the same source of fine aggregate. Required pavement thickness varies significantly with different fine aggregate sources. The use of sand B basically requires the pavement with all other properties the same to be much thicker.

Table 10 Effect Due to Different Sources of Sand

sand A, Southern WI		sand B, Western WI	
Mix#	Thickness, in	Mix#	Thickness, in
31	8.4	96	9.4
32	9.1	97	9.9
37	8.6	98	8.6
76	9.0	101	9.1
77	8.4	102	8.6
78	8.0	103	8.5
81	9.3	106	9.1
82	8.3	107	9.6
83	8.0	108	8.4
72	8.6	92	8.3
73	7.8	93	8.8

4. Effects on Pavement Thicknesses due to Different Hierarchical Strength Input Options

The use of different hierarchical levels of inputs was expected to affect the predicted pavement performances (reflected by critical pavement thicknesses) by MEPDG. Detailed descriptions of the three levels of input options are shown in Appendix B. Laboratory modulus of elasticity test results, flexural strength test results, and compressive strength test results on the same selected concrete mixes were substituted into the trial pavement design (shown in Appendix C) using MEPDG to obtain the required pavement thickness each corresponding to level 1, level 2, and level 3 option, shown in Table 11.

Table 11 Effect due to Different Levels of Strength Input Options

	Thickness, in		
Mix #	Level 1	Level 2	Level 3
1	9.32	9.30	9.29
2	8.94	9.75	9.74
3	8.45	9.79	9.75
4	9.51	9.28	9.29
5	8.40	9.10	9.09
6	9.05	9.85	9.84
7	8.91	9.59	9.59
8	8.70	8.90	8.89
9	8.05	8.86	8.83
10	8.49	9.31	9.30
11	8.57	9.30	9.30
12	9.50	9.56	9.55
13	8.66	9.09	9.06
14	8.99	9.27	9.24
15	8.60	9.01	9.01

It is observed from Table 11 that in most cases, the use of the level 2 option provides very conservative results compared to the ones provided by the level 1 option, yet almost the same results as the ones obtained from the level 3 option. This phenomenon illustrates that the empirical relations within level 2 option lead to conservative pavement designs for concrete made with Wisconsin materials. However, the empirical relation within level 3 option to convert the 28-day modulus of rupture to modulus of rupture values at any time basically coincides with the test results of concrete compressive strength.

5. MEPDG Software's Limitations

The default empirical relations within MEPDG result in significant limitations on certain variables' ranges. For example, the concrete's flexural strength input is restrained within the range from 0 to 950psi, as this upper limit corresponds to a converted compressive strength of 1,000,000 psi, the threshold for concrete compressive strength. Any flexural strength inputs greater than 950psi result in a system error of exceeding the compressive strength limit, preventing the software from running. However, based on the observation of laboratory test results, it is possible for concrete 90-day flexural strength to exceed 950 psi.

Furthermore, MEPDG software does not consider the effect of using slag or fly ash as a supplement for cement. The shrinkage calculation is only relevant to cement properties such as cement content and cement type. When slag or fly ash is added in the concrete mix, the shrinkage is expected to

be different. In the section analyzing the slag and fly ash's effects on pavement performances, only their effects on concrete strength and thermal properties are considered. In reality, the use of slag and fly ash should also affect the shrinkage properties of concrete pavements.

Summary

1. The most sensitive inputs of MEPDG for JPCP new design are PCC's modulus of rupture (MR), PCC's modulus of elasticity (E), PCC's compressive strength (fc'), PCC's coefficient of thermal expansion (α), and PCC's unit weight (ρ).
2. It is reasonable that variables of MR, E, α, and fc' were identified sensitive. However, it is suspected that the effect of ρ is overestimated by MEPDG. The significant benefits reflected in JPCP design using MEPDG due to the use of the widened slab are also suspicious.
3. The detailed inputs required for the level 1 option are treated as independent variables with very specific calculation purposes. The interrelationship between the concrete strength inputs and concrete component properties are not addressed directly within the program and must be established by laboratory testing.
4. Pavements using concrete mixed with basalt or granite coarse aggregates tend to have the best predicted performances by MEPDG. On the contrary, quartzite coarse aggregate leads to the worst predicted performances by MEPDG. The use of slag or fly ash as supplementary cementitious material could significantly improve the predicted pavement performances.
5. The use of the level 2 input option leads to very conservative pavement designs compared to the level 1 option. However, the difference between the results obtained from the level 2 input option and the level 3 input option is negligible.
6. The allowable range for concrete modulus of rupture input within MEPDG is not applicable for concrete mixed with Wisconsin materials.

Reference

1. Guide for Mechanistic-Empirical Design of New and Rehabilitated Pavement Structures. Final Report. National Cooperative Highway Research Program, Transportation Research Board, National Research Council, 2004
2. Tarun R. Naik, Yoon-moon Chun, and Rudolph N. Kraus, "Investigation of Concrete Properties to Support Implementation of the New AASHTO Pavement Design Guide". Final Report. WHRP 06-14. Wisconsin Department of Transportation, 2006.
3. Ruipeng Li: Sensitivity Analysis of 2002 MEPDG Strength Inputs and Evaluation of Concrete CTE Using Wisconsin Materials. Wisconsin Highway Research Program, Madison, Wisconsin, 2011

Appendix ADetailed Inputs Description for MEPDG

Inputs required for New Rigid Pavement design

- General Information
- Site/Project identification
- Analysis Parameters
- Traffic
- Climate
- Pavement Structure
- Design Feature

General Information includes the following parameters: design life, construction month, traffic opening month, pavement type (JPCP or CRCP).

Site/Project Identification includes project location and project identification (Project ID, Section ID, begin and end mile posts, traffic direction).

Analysis Parameters include initial IRI and performance criteria, i.e.,

For JPCP
Transverse cracking: allowable 10~45%
Transverse joint faulting: allowable 0.1~0.2 inch
Smoothness: typical terminal IRI 150~250 in/mile

For CRCP
Crack Width and Crack LTE: Crack width in cold weather is most critical parameter. Crack LTE is the ultimate strength parameter and depends on crack width and number of heavy axles applied, which should be limited to more than 95% throughout the design life.
Punchouts: defines the number of punchouts per mile, typically 10~20/mile
Smoothness: typical terminal IRI 150~250 in/mile

Inputs required for traffic characterization

- Traffic volume-base year information
  - Two-way annual average daily truck traffic (AADTT)
  - Number of lanes in the design direction
  - Percent trucks in design direction
  - Percent trucks in design lane
  - Vehicle (truck) operational speed
- Traffic volume adjustment factors
  - Monthly adjustment
  - Vehicle class distribution
  - Hourly truck distribution
  - Traffic growth factors
- Axle load distribution factors

- General traffic inputs
  - Number axles/trucks
  - Axle configuration
  - Wheel base

Inputs required for climate include water table depth and climate data from specific weather station corresponding to the project site.

Inputs required for pavement structure and design feature include the trial thickness for each layer and material characteristics.

Materials Category	Materials Inputs Required		
	Materials Inputs for critical response computations	Additional materials inputs required for distress/transfer functions	Additional materials inputs required for climatic modeling
PCC Materials (surface layer only)	Static modulus of elasticity adjusted with time; Poisson's ratio; Unit weight; Coefficient of thermal expansion;	Modulus of rupture; Split tensile strength; Compressive strength; Cement type; Cement content; w/c ratio; ultimate shrinkage; amount of reversible shrinkage;	Surface shortwave absorptivity; Thermal conductivity; Heat capacity;
Chemically Stabilized Materials (lean concrete, cement treated, soil cement, lime-cement-flyash, lime-flyash, lime stabilized layers)	Resilient modulus for lime stabilized soil; Elastic modulus for the rest types; Poisson's ratio; Unit weight;	Flexible design (minimum resilient modulus, modulus of rupture); Rigid design (base erodibility);	Thermal conductivity; Heat capacity
Unbound Base/Subbase and Subgrade Materials	Seasonally adjusted resilient modulus (Mr); Poisson's ratio; Unit weight; Coefficient of lateral pressure;	Gradation parameters Base erodibility (for rigid design);	Plasticity index; Gradation parameters; Effective grain sizes; Specific gravity; Saturated hydraulic conductivity; Optimum moisture contents; Parameters to define soil water characteristic curve;
Recycled Concrete Materials-Fractured PCC Slabs	Resilient Modulus; Poisson's ratio;	Base erodibility (for rigid design)	Thermal conductivity; Heat capacity;
Bedrock	Elastic modulus; Poisson's ratio; Unit weight;	None;	None;

Appendix BHierarchical Strength Inputs of PCC Layer for JPCP New Design

PCC Modulus Characterization for New/Reconstruction JPCP and CRCP and PCC overlays

Input Level	Description
1	• PCC modulus of elasticity, Ec, is determined directly by laboratory testing. Chord modulus from ASTM C 469 at 7, 14, 28, 90 days • Estimate 20-year to 28-day (long-term) elastic modulus ratio • Develop modulus gain curve using the test data and long-term modulus ratio to predict Ec at any time in design life
2	• Ec determined indirectly from compressive testing at 7, 14, 28, 90 days. f_c' from AASHTO T22, or enter Ec directly • Estimate 20-year to 28-day compressive strength ratio • $E_C=33\rho^{3/2} f_c'^{1/2}$ psi • Develop modulus gain curve using the test data and long-term modulus ratio to predict Ec at any time in design life
3	• E_C determined from 28-day estimates of flexural strength (MR) or f_c', MR from AASHTO T97 or historical records, f_c' from AASHTO T22 or historical records, or enter Ec directly • Estimate a 28-day MR value, $MR(t) = (1 + log_{10}\left(\frac{t}{0.0767}\right) - 0.01566 \log_{10}\left(\frac{t}{0.0767}\right)^2) \cdot MR_{28-day}$ • Estimate Ec(t) by $f_c'(t)$ from MR(t) $f_c'=(MR/9.5)^2$ psi $E_C=33\rho^{3/2} (fc')^{1/2}$ psi • If a 28-day f_c' is estimated, first convert it to MR, then project MR(t), then Ec(t)

(The modulus gain over time is considered directly to calculate accumulation of incremental damage over time.)

Poisson's ratio of PCC Materials

Level 1: determined with elastic modulus, ASTM C 469
Level 2: not applicable
Level 3: Poisson's ratio for normal concrete typically ranges between 0.11 and 0.21, 0.15~0.18 are typically assumed for PCC design

PCC Flexural Strength Characterization for new or Reconstruction JPCP and CRCP and PCC overlays

Input Level	Description
1	• PCC MR will be determined directly by laboratory testing using the AASHTO T 97 protocol at 7, 14, 28, 90-days. (specimen prepared and cured from AASHTO T23, T24, T126 • Estimate 20-year to 28-day MR ratio (max=1.2) • Develop strength gain curve $\frac{MR(t)}{MR(28-day)} = \propto_1 + \propto_2 \log_{10}(AGE) + \propto_3 [\log_{10}(AGE)]^2$ AGE: year;
2	• MR determined indirectly from f_c' at 7, 14, 28, 90-days using AASHTO T22 • Estimate 20-year to 28-day compressive strength ratio (max=1.35, or 1.2 for relative low humidity) • Develop compressive strength gain curve at any time • MR=9.5*(f_c')$^{1/2}$ psi
3	• MR(t) determined from 28-day MR (AASHTO T97 or records) or f_c' (AASHTO T22 or records) • If start from 28-day MR $\frac{MR(t)}{MR(28-day)} = 1.0 + 0.12\log_{10}(AGE/0.0767) - 0.01566[\log_{10}(AGE/0.0767)]^2$ • If start from 28-day f_c', convert it to 28-day MR, follow the same steps

PCC indirect tensile strength for new and reconstruction CRCP projects and CRCP overlays

Estimating PCC Indirect Tensile Strength at Input Level 1

Input Parameter	Required Test Data				Ratio of 20-year/28-day modulus (max1.2)	Test Procedule
	7-day	14-day	28-day	90-day		
ft	y	y	y	y	y	AASHTO T198

Estimating PCC Indirect Tensile Strength at Input Level 2

Input Parameter	Required Test Data				Ratio of 20-year to 28-day Strength	Recommended Test Procedure
	7-day	14-day	28-day	90-day		
Compressive strength	y	y	y	y	y	AASHTO T22

Step 1: Input compressive strength results at 7, 14, 28,90 days and the estimated 20-year to 28-day ratio. Maximum value of 20-year to 28-day ratio, 1.35 or 1.20 for relatively low humidity, or determined by historical data

Step 2: develop strength gain curve

Step 3: $f_c'(t)$ is converted into MR(t) by the above equation. Then MR(t) is converted to ft by the relation: ft=0.67MR

Estimating PCC Elastic Modulus at Input Level 3

Input either 28-day compressive or flexural strength result

Input Parameter	28-day value	Recommended Test Procedule
Flexural Strength	y	AASHTO T97 or from records
Compressive Strength	y	AASHTO T22 or from records

Appendix C Sample Inputs for Sensitivity Analysis

	Input Parameter	Value
General	Design life (years)	30
	Initial IRI (in/mile)	75
	Terminal IRI (in/mile)	250 (95% reliability)
	Transverse cracking (% slabs cracked)	15 (95% reliability)
	Mean joint faulting (in)	0. 2 (95% reliability)
Traffic	Initial two-way AADTT	2500
	Number of lanes in design direction	2
	Percent of trucks in design direction (%)	50
	Percent of trucks in design lane (%)	95
	Operational speed (mph)	60
	Mean wheel location (in)	18
	Traffic wander standard deviation (in)	10
	Design lane width (ft)	12
	Traffic adjustment factors	Default
Climate	Climatic Region	Madison, Wisconsin
	Water Table Depth (ft)	5
Pavement Structure	Permanent curl / warp temperature difference (°F)	-10
	Joint Spacing (ft)	15
	Sealant type	None
	Dowel Diameter (in)	1.25
	Dowel Bar Spacing (in)	12
	Edge Support	None
	Erodibility Index	Fairly Erodable (4)
	Loss of full friction (months)	240
	PCC-Base Interface	Full friction
	Surface Shortwave absorptivity	0.85
PCC Layer	Slab thickness (in)	10
	Unit Weight (pcf)	147.5
	Poisson's Ratio	0.2
	Coefficient of thermal expansion (με/°F)	5.70
	Thermal conductivity (BTU/hr-ft-°F)	1.25
	Heat capacity (BTU/lb-°F)	0.28
	Cement type	Type I
	Cementitious material content (lb/yd^3)	565
	Water/cement ratio	0.4
	Aggregate Type	Granite
	Reversible shrinkage (% of ultimate shrinkage)	50
	Time to develop 50% of ultimate shrinkage (days)	35
	Curing method	Curing Compound
	28-day PCC Compressive Strength (psi)	4800 (level 3)
Base Layer	Unbound Material	Crushed Stone
	Layer Thickness (in)	6
	Modulus (psi)	30000
Sub-base Layer	Unbound Material	River-run Gravel
	Layer Thickness (in)	4
	Modulus (psi)	20000
Subgrade Layer	Unbound Material	A-6
	Layer Thickness (in)	Semi-infinite
	Modulus (psi)	14000

Appendix D Curve Fitting Analysis

Based on the analysis on the relation of y vs. x data points, its approximation curve is similar to the shape of an exponent function for most of the variables. However, for certain insensitive variables, y barely changes with the change of x values, where a linear relation with a very small slope may more accurately reflect this relation. Therefore, two approximation curves are proposed here, which are $= A \cdot B^x + C \cdot x + D$, a hybrid form combined with unknown exponent term and unknown linear term, and $y = A \cdot B^x + D$, an exponent function form. Comparisons were conducted between these two fitting curves and a more accurate one was selected as the fitting curve for each of the variables used for sensitivity analysis.

Shown from Figure D-1 to Figure D-3, for both sensitive variables (AADTT and fc') and insensitive variable (Poisson's Ratio), the fitting line $y = A \cdot B^x + D$ (black line shown in each figure) has a higher approximation. Therefore, it is selected as the fitting curve to simulate the relation of y vs. x for each of the variables selected for sensitivity analysis.

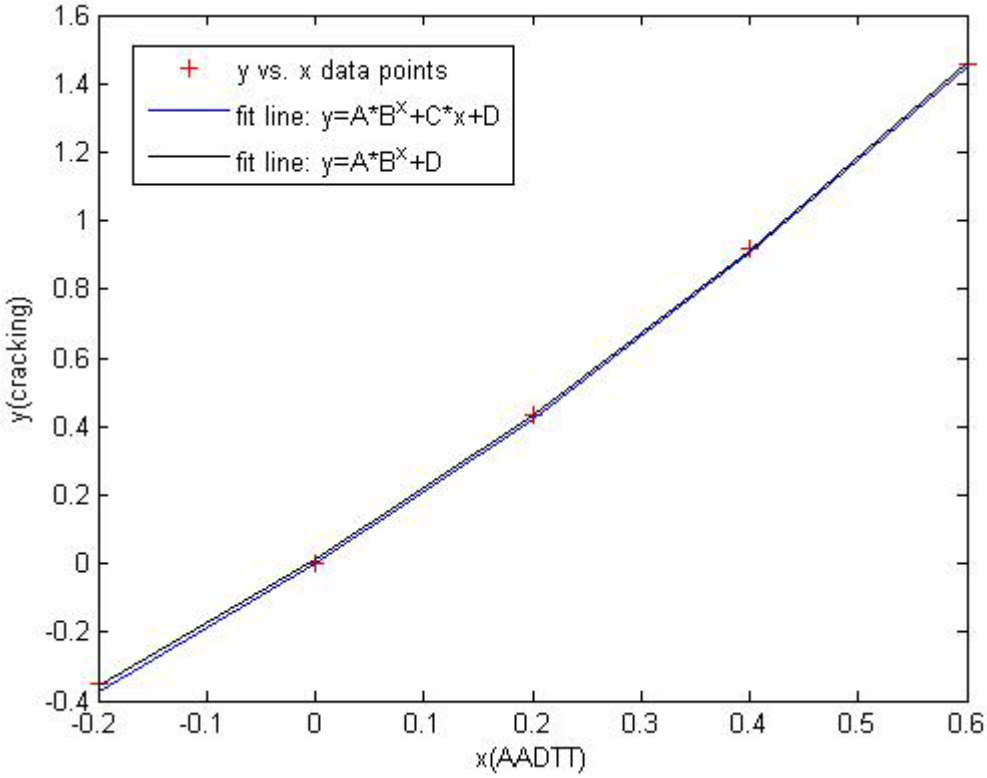

Figure D-1 Comparisons for Two Fitting Lines for the Relation of Cracking vs. AADTT

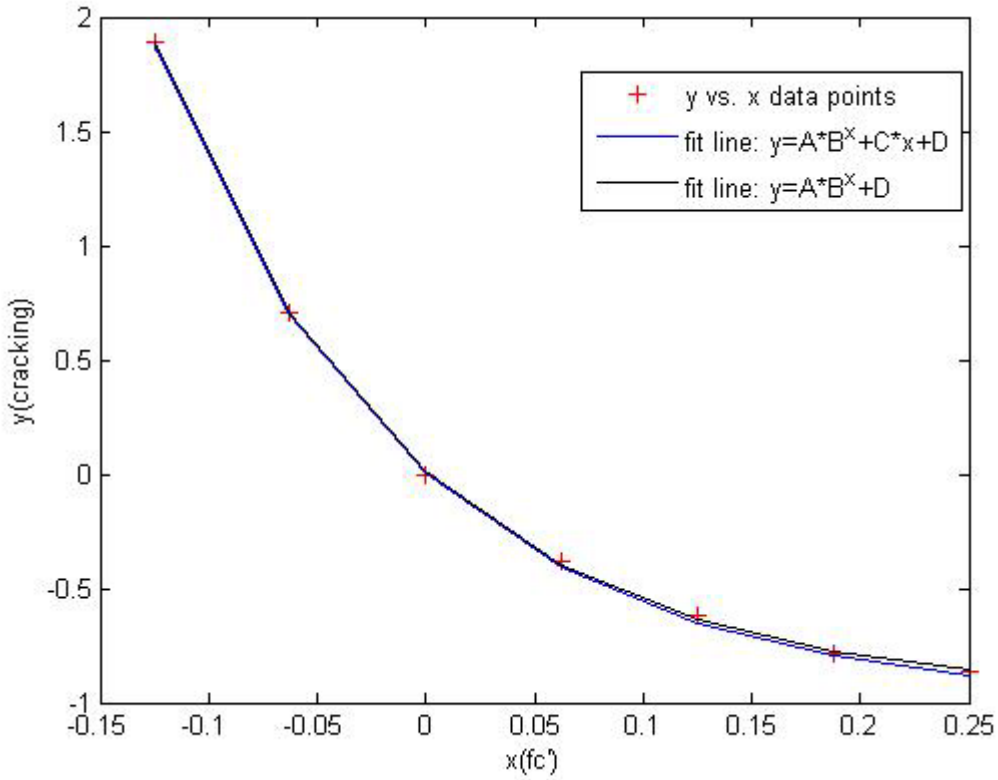

Figure D-2 Comparisons for Two Fitting Lines for the Relation of Cracking vs. fc'

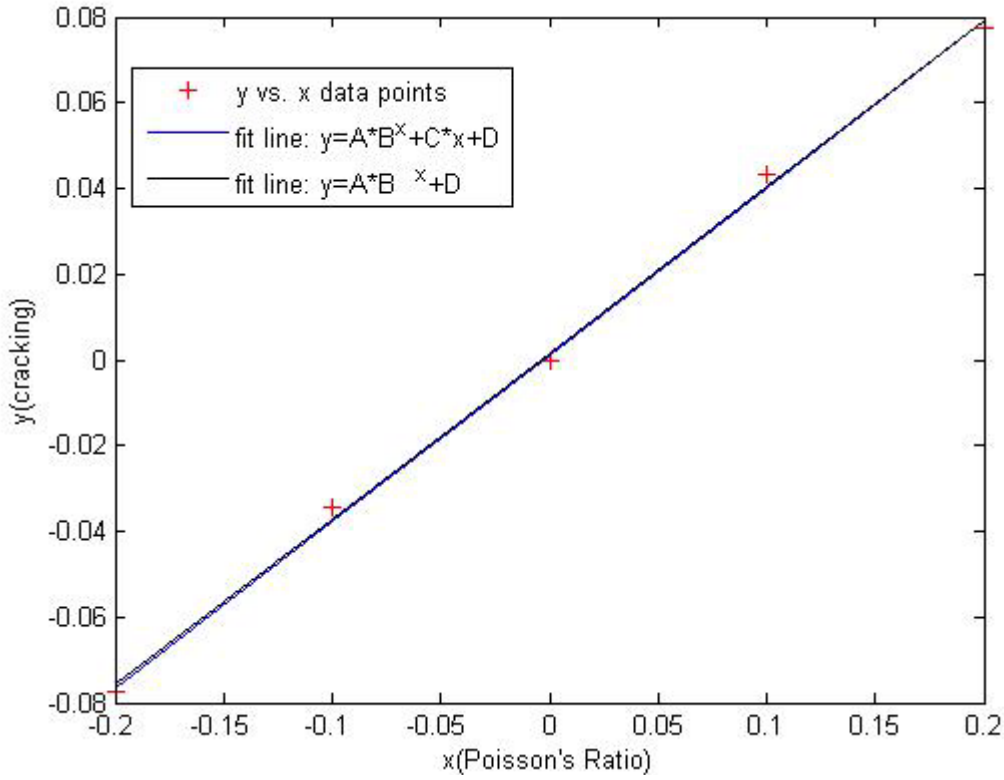

Figure D-3 Comparisons for Two Fitting Lines for the Relation of Faulting vs. Poisson's Ratio

CFIRE

University of Wisconsin-Madison
Department of Civil and Environmental Engineering
1410 Engineering Drive, Room 270
Madison, WI 53706
Phone: 608-263-3175
Fax: 608-263-2512
cfire.wistrans.org